CARPATHIAN JOURNAL OF FOOD SCIENCE AND TECHNOLOGY

journal homepage: **http://chimie-biologie.ubm.ro/carpathian_journal/index.html**

Research article

PREPARATION, OPTIMIZATION AND APPLICATION OF GINGEROL MICROCAPSULES FOR FRESH BEEF PRESERVATION

Nannan Wu[1], Haoran Sun[1], Shougang Jiang[1,2,3,4,5]✉, Dayu Peng[1], Siyan Zhang[1,2,3,4,5], Qi Meng[1,2,3,4,5], Yunzhu Tian[1,2,3,4,5]

[1]College of Chemistry Chemical Engineering and Resource Utilization, Northeast Forestry University, Harbin, P.R. China

[2]State Engineering Laboratory of Bio-Resources Eco-Utilization, Northeast Forestry University, Harbin, P.R. China

[3]Key Laboratory of Forest Plant Ecology, Ministry of Education, Northeast Forestry University, Harbin, P.R. China

[4]Heilongjiang Provincial Key Laboratory of ecological utilization of Forestry-based active substances, Harbin, P.R. China

[5]State Key Laboratory of Utilization of Woody Oil Resource, Harbin, P.R. China

✉395622044@qq.com, ORCID Number 0000-0001-7868-9600

https://doi.org/10.34302/crpjfst/2025.17.2.11

Article history:
Received:
May 7th, 2025
Accepted:
July 23rd, 2025

Keywords
Gingerol;
Microencapsulation;
Spray drying;
Response surface methodology;
Beef preservation.

ABSTRACT

To address the challenges of instability and poor water solubility associated with gingerol as a food preservative, this study developed gingerol microcapsules using a composite wall material consisting of arabic gum (GA) and whey protein isolate (WPI) through a spray-drying technique. The physicochemical properties of the microcapsules were thoroughly investigated, and their efficacy in preserving fresh beef was evaluated. The microencapsulation conditions were optimized using response surface methodology (RSM), yielding optimal parameters as follows: wall-to-core ratio of 5.103:1 (w/w), solid content of 8.912% (wt%), GA content of 54.916% (wt%), and emulsifier content of 1.019% (wt%). Under these optimized conditions, the encapsulation efficiency of gingerol reached 71.83%, and the microcapsules demonstrated superior water solubility (94.58%). Stability and antioxidant activity assessments revealed that the microcapsules exhibited enhanced stability and antioxidant properties compared to free gingerol. Preservation tests on fresh beef indicated that the gingerol microcapsules effectively extended the shelf life of beef by 72-96 hours at room temperature. These findings suggest that gingerol microcapsules hold significant potential as a natural preservative in the food industry.

1. Introduction

Gingerol, a bioactive phenolic compound derived from ginger rhizomes (*Zingiber officinale Roscoe*), has attracted considerable scientific interest owing to its diverse biological properties, including antioxidant,

antimicrobial, and anti-inflammatory activities (Kamaruddin *et al.*, 2013). The compound demonstrates remarkable antibacterial efficacy against various foodborne pathogens, such as Escherichia coli, Salmonella spp., and Staphylococcus aureus (Ghasemzadeh et al., 2018), making it particularly valuable for application in perishable food products, especially meat and meat derivatives. Gingerol not only mitigates microbial-induced spoilage but also extends the shelf life of these products through its dual functionality.

The antioxidant capacity of gingerol plays a crucial role in meat preservation by inhibiting lipid peroxidation, maintaining sensory attributes (including color and flavor profiles), and preventing oxidative deterioration of fats (Ivane et al., 2022). In the context of increasing consumer demand for natural food additives and stringent food safety regulations, natural preservatives like gingerol have emerged as a significant research focus in food science. For instance, studies have demonstrated that ginger essential oil effectively suppresses microbial proliferation, inhibits malondialdehyde formation, reduces volatile basic nitrogen production, and stabilizes pH in preserved duck breast meat (Chen et al., 2024). As a natural, eco-friendly preservative, gingerol presents a viable alternative to synthetic chemical preservatives while meeting contemporary food safety standards (Laelago et al., 2023).

However, the practical application of gingerol faces several challenges. The compound exhibits thermal and photolability, undergoing degradation when exposed to ultraviolet radiation, atmospheric oxygen, or elevated temperatures, which significantly diminishes its bioactivity (Ahad et al.,2023; Sang *et al.*, 2020).

Furthermore, its lipophilic nature and rapid metabolism in the gastrointestinal tract result in limited bioavailability and increased storage and transportation costs. These limitations necessitate the development of effective stabilization strategies to fully exploit gingerol's potential in food applications.

Microencapsulation technology has emerged as a promising approach to address these limitations. This technique not only enhances the stability and bioavailability of gingerol but also facilitates controlled release, thereby maintaining moisture content, reducing water loss in beef during refrigeration, and preserving meat quality attributes (Al-Hamayda et al., 2023). Among various encapsulation methods, spray-drying technology has gained prominence due to its operational simplicity, cost-effectiveness, high efficiency, and suitability for heat-sensitive compounds (Setyaningsih et al., 2020). The process yields powdered formulations that offer advantages in transportation, storage, and application.

The selection of appropriate wall materials is critical in determining the physicochemical properties of the encapsulated product, including particle morphology, size distribution, flow characteristics, and storage stability (Rialita et al., 2018). Proteins and polysaccharides exhibit distinct encapsulation capabilities, with protein-based matrices demonstrating superior oil encapsulation but higher moisture sensitivity, while polysaccharide-based materials offer enhanced water retention and mechanical stability (Xu et al., 2023). Whey protein isolate (WPI) has been identified as an optimal encapsulation matrix due to its excellent emulsifying properties, water solubility, biocompatibility, and thermal stability (Kalajahi et al., 2023). The combination of WPI with gum arabic (GA) has been shown to improve microcapsule integrity, enhance environmental stress tolerance, and optimize powder characteristics by forming more compact structures with reduced hygroscopicity and improved flow properties (Zhang et al., 2022).

In this investigation, we optimized the formulation of gingerol emulsion through systematic evaluation of core-wall ratio, GA proportion, solid content, and emulsifier concentration. Response surface methodology (RSM) was employed to determine optimal encapsulation efficiency. Comprehensive characterization of the microcapsules included analysis of particle size, morphological features, storage stability, and free radical scavenging

capacity. Furthermore, we evaluated the practical application of gingerol microcapsules in fresh beef preservation, demonstrating their efficacy in extending product shelf life and providing a viable solution for natural meat preservation.

2. Materials and methods

2.1. Chemicals and reagents

Gingerols (purity ≥50%) were procured from Guangzhou Jingjing Biotechnology Co., Ltd. (Guangdong, China). Whey protein isolate (WPI, purity ≥90%) was sourced from Fonterra Trading (Shanghai) Co., Ltd. (Shanghai, China). Gum Arabic (GA) was supplied by Dezhou Huiyang Biotechnology Co., Ltd. (Shandong, China). Modified soybean phospholipid was obtained from Henan Siwei Biotechnology Co., Ltd. (Henan, China). Sulfuric acid standard titration solution (0.1010 mol/L) was provided by Temo Quality Inspection Standard Material Center (Beijing, China). Additional reagents, including pepsin (1:30000), trypsin (1:250), bromocresol green (≥95%), and methyl red (≥95%), were purchased from Shanghai Yuanye Bio-Technology Co., Ltd. (Shanghai, China). 2,2'-Azino-bis(3-ethylbenzothiazoline-6-sulfonic acid) diammonium salt (ABTS, 98%) and 2,2-diphenyl-1-picrylhydrazyl (DPPH, 96%) were acquired from Shanghai Macklin Biochemical Co., Ltd. (Shanghai, China). Dipotassium hydrogen phosphate (≥99.5%), ethanol (≥99.8%), and magnesium oxide (≥98%) were supplied by Shanghai Aladdin Biochemical Technology Co., Ltd. (Shanghai, China). Sodium hydroxide (≥95%) was obtained from Tianjin Continental Chemical Reagent Factory (Tianjin, China).

2.2. Optimization of gingerol microcapsule processing and spray drying

Whey protein isolate (WPI) and gum arabic (GA) were combined to form the composite wall material, with GA constituting 45% of the total wall material and a solid content of 10%. The composite wall material was dissolved in warm water at 50°C under continuous stirring until complete dissolution was achieved. Gingerol was then incorporated into the wall material solution at a fixed core-to-wall ratio of 1:5, and modified soybean lecithin was added at a concentration of 4%. The mixture was homogenized using a high-speed stirrer to ensure uniform dispersion (Ahad et al., 2023).

Table 1. Coded factor levels for response surface experimental design

Factor	Unit	Code	Level		
			-1	0	1
Wall-to-core ratio	(w/w)	A	4:1	5:1	6:1
Solid content	(wt%)	B	5	10	15
Gum arabic content	(wt %)	C	45	55	65
Emulsifier content	(wt %)	D	0	1	2

Spray drying was conducted using a spray dryer equipped with a 0.7 mm nozzle diameter (B-290 Small Spray Dryer, Büchi Labortechnik AG, Flawil, Switzerland). Consistent spray

drying parameters were maintained for all emulsions: an inlet air temperature of 165°C, an outlet temperature of 90°C, a peristaltic pump feeding rate of 11.7 mL/min, a nozzle cleaner setting of level 2, a pumping rate of 100%, and an airflow meter setting of 35 mm.

To optimize the microencapsulation process, a single-factor experiment was initially performed (Nguyen et al., 2024). Based on the results of the single-factor experiment, a Box-Behnken design (BBD) with four factors and three levels was employed to determine the optimal preparation conditions for achieving the highest encapsulation efficiency. The effects of four independent variables on the encapsulation efficiency of gingerol (FOEE (Y)) were investigated: (A) wall-to-core material ratio, (B) solid content, (C) GA content, and (D) emulsifier content. The experimental design incorporated three coded levels (−1, 0, and +1) for each variable, and a total of 29 experimental runs were conducted. All experiments were performed in triplicate to ensure reproducibility and reliability of the results. The specific coded factor levels of the experimental variables are presented in Table 1.

2.3. Determination of microcapsule encapsulation efficiency

The encapsulation efficiency (EE) of gingerol microcapsules was determined following the methodology (Ahad et al., 2024), using the following equation:

EE % = 1- (surface gingerol content of microcapsules / total gingerol content in microcapsules) × 100 (1)

2.4. Powder yield

The powder yield refers to the mass percentage of microcapsule powder obtained from the spray-drying process relative to the total solid content (comprising both wall and core materials) present in the initial emulsion (Ahad et al., 2021). The powder yield was calculated using the following equation:

Powder yield % = Mass of microcapsule powder collected from the spray dryer / Total solid mass in the sample feed solution × 100 (2)

2.5. Physical properties of gingerol microcapsules

2.5.1 Moisture content

The moisture content of the microcapsules was determined using a gravimetric method. The microcapsule powder was dried in a hot air oven at 105°C until a constant weight was attained. The moisture content was calculated based on the mass difference of the sample before and after the drying process, expressed as a percentage of the initial sample weight.

2.5.2 Solubility

The solubility of the microcapsule powder was determined according to the method described by Zhang et al. (Zhang et al., 2022), with slight modifications. Briefly, a measured quantity of gingerol microcapsule powder was dissolved in deionized water at 25°C. The solution was centrifuged at 4000 rpm for 10 minutes, and the supernatant was carefully discarded. The undissolved residue was resuspended in an equivalent volume of deionized water, vigorously shaken to ensure complete suspension of the precipitate, and centrifuged again under the same conditions. After discarding the supernatant, the precipitate was transferred to a pre-weighed dish and dried at 105°C until a constant weight was achieved.

The solubility (S) was calculated using the following equation:

S % = {1 - (total mass of undissolved residue and weighing dish - mass of empty weighing dish) / initial mass of the sample} × 100 (3)

2.5.3 Zeta potential, Polydispersity index, and Particle size distribution

The Zeta potential (ζ-potential), polydispersity index (PDI), and particle size distribution of the microcapsules were determined using a dynamic light scattering (DLS) analyzer (NANOTRAC Wave II, Microtrac MRB, USA). The gingerol

microcapsule powder was dispersed in distilled water at a ratio of 1:80 (w/v) and homogenized by gentle stirring with a magnetic stirrer at room temperature (25 ± 1°C) to obtain a uniform suspension. Subsequently, the prepared suspension was introduced dropwise into the sample cell for analysis.

2.6. Structure characterization of gingerol microcapsules

2.6.1 Fourier transform infrared (FTIR) spectroscopy analysis

The FTIR spectra of Arabic gum (AG), whey protein isolate (WPI), and gingerol microcapsule powder were acquired following the method outlined by Wang et al. (Wang et al., 2021), with slight modifications. Briefly, AG, WPI, and microcapsule samples were individually mixed with potassium bromide (KBr) powder at a mass ratio of 1:100 (sample:KBr). The mixtures were homogenized by thorough grinding to ensure uniformity. Transparent pellets were prepared by compressing the mixtures using a hydraulic pellet press. The resulting pellets were placed in the sample holder of a Nicolet Summit FT-IR spectrometer (Thermo Fisher Scientific, USA) and analyzed within a wavenumber range of 400–4000 cm^{-1}. Each spectrum was recorded as an average of 32 scans to ensure optimal signal-to-noise ratio.

2.6.2 X-ray diffraction (XRD) analysis

The crystalline structures of gingerol microcapsules, Arabic gum (AG), and whey protein isolate (WPI) were characterized using an X-ray diffraction (XRD) analyzer. Each sample was finely ground and uniformly dispersed onto a glass slide, followed by compression into a thin, homogeneous layer. The prepared sample was mounted on the sample holder and subjected to X-ray irradiation generated from a Cu-Kα radiation source (λ = 1.5406 Å). The XRD patterns were recorded over a 2θ scanning range of 10° to 60° at a scan speed of 2°/min.

2.6.3 Scanning electron microscopy (SEM)

The dried microcapsule samples were affixed onto sample holders using conductive adhesive and subsequently sputter-coated with a thin layer of gold to enhance conductivity. The surface morphology of the gingerol microcapsule powder was examined using a Nano Apreo 2 C scanning electron microscope (Thermo Fisher Scientific, Waltham, Massachusetts, USA). The SEM images were acquired at an accelerating voltage of 15 kV under high vacuum conditions.

2.7. Storage stability analysis

The storage stability of the microcapsules was evaluated according to the method reported by Devi et al. (2023), with slight modifications. Briefly, a measured quantity of gingerol and microcapsule powder was accurately weighed and stored under four distinct environmental conditions: (1) 25°C with exposure to natural light, (2) 25°C in the dark, (3) 4°C with exposure to natural light, and (4) 4°C in the dark. The gingerol content in the samples was quantified at 3-day intervals over a total storage period of 12 days to investigate the effects of temperature and light exposure on the encapsulation stability.

The retention rate of gingerol (R, %) was calculated using the following equation:

$$R\ \% = \text{Residual gingerol content on day n} / \text{Initial gingerol content} \times 100 \quad (4)$$

2.8. Antioxidant activity evaluation

2.8.1 DPPH Radical Scavenging Activity

The DPPH radical scavenging activity was assessed according to an optimized method reported by Yang et al. (2022). Briefly, gingerol and spray-dried microcapsule samples were dissolved in anhydrous ethanol to prepare solutions with gingerol concentrations ranging from 0.1 to 0.6 mg/mL. A 2 mL aliquot of each sample solution was mixed with 2 mL of 0.2 mM DPPH ethanol solution. The mixture was incubated in the dark at room temperature (25 ± 1°C) for 30 minutes. The absorbance of the resulting solution was measured at 517 nm using a UV-Vis spectrophotometer (UV-3900, Hitachi, Japan). A control group (sample solution without DPPH) and a blank group

(DPPH solution without sample) were included for comparison.

The DPPH radical scavenging rate (R, %) was calculated using the following equation:

$$R\ \% = \{1 - (\text{absorbance value of the sample group} - \text{absorbance value of the control group}) / \text{absorbance value of the blank group}\} \times 100 \quad (5)$$

2.8.2 Evaluation of ABTS+ Radical Scavenging Activity

The $ABTS^+$ radical scavenging activity was determined following the method outlined by Rahim et al. (2023), with slight modifications. The $ABTS^+$ working solution was prepared by mixing a 7 mM ABTS aqueous solution with a 2.45 mM potassium persulfate ($K_2S_2O_8$) solution, followed by incubation in the dark at room temperature (25 ± 1°C) for 16 hours. The solution was subsequently diluted with anhydrous ethanol to achieve an absorbance of 0.7 ± 0.02 at 734 nm. Gingerol and spray-dried microcapsule samples were dissolved in anhydrous ethanol to obtain solutions with gingerol concentrations ranging from 0.1 to 0.6 mg/mL. A 50 µL aliquot of each sample solution was mixed with 950 µL of the $ABTS^+$ working solution, and the mixture was incubated in the dark for 20 minutes. The absorbance of the reaction mixture was measured at 734 nm using a UV-Vis spectrophotometer. A control group (sample solution without $ABTS^+$ working solution) and a blank group ($ABTS^+$ working solution without sample) were included for comparison. The $ABTS^+$ radical scavenging rate was calculated using Equation (5).

2.9. Application of gingerol microcapsules in the preservation of fresh beef

Fresh beef was prepared under sterile conditions by removing fat and connective tissue and cutting it into uniform cubes (3 cm × 3 cm × 1 cm). The experiment comprised three treatment groups (M_1–M_3) and one control group (M_0), as follows: M_0: Treated with sterile water. M_1: Fully immersed in a solution of blank microcapsules (without gingerol). M_2: Treated with gingerol crude oil at a concentration equivalent to the gingerol content in the microcapsules. M_3: Fully immersed in a gingerol microcapsule solution. The treated beef samples were placed in sterile food preservation bags and stored at 4°C ± 1°C. Every 3 days, three samples were randomly selected for analysis of pH, total plate count (APC), total volatile basic nitrogen (TVB-N), and color parameters.

2.9.1 pH measurement

Two grams of beef were homogenized with 25 mL of deionized water using a high-speed homogenizer (FSH-2A, China) (Lian et al., 2023). The pH of the homogenate was measured at 25°C using a calibrated digital pH meter (PB-10, Sartorius, Germany). Measurements were performed in triplicate to ensure reproducibility.

2.9.2 Aerobic plate count (APC)

Two grams of beef were homogenized with 20 mL of sterile saline solution. The homogenate was serially diluted (1:10 to 1:100) with sterile saline. A 1 mL aliquot of the diluted homogenate (with 1 mL sterile water as a control) was transferred to a sterile Petri dish and mixed with 15–20 mL of plate-count agar medium. The Petri dishes were gently rotated to ensure uniform distribution of the sample, followed by solidification of the agar. The plates were inverted and incubated at 37°C for 48 hours. Colony-forming units (CFU) were enumerated and expressed as CFU/g of beef (Wang et al., 2025).

2.9.3 Total volatile basic nitrogen (TVB-N)

The total volatile basic nitrogen (TVB-N) content was determined using an automatic Kjeldahl nitrogen analyzer (K9860, Hainuo Instrument Co., China). A sulfuric acid titrant (0.1010 mol/L) was used as the standard solution. Briefly, 10 g of beef was minced and mechanically homogenized, then transferred to a conical flask containing 100 mL of distilled water. The mixture was agitated to achieve homogeneous dispersion and incubated for 30 minutes at room temperature. The suspension was filtered through Whatman No. 1 filter paper, and 10 mL of the filtrate was quantitatively transferred to a digestion tube.

Subsequently, 1.0 g of magnesium oxide (MgO) was added, and the sample underwent steam distillation followed by titration with the standardized sulfuric acid solution (Huang et al., 2012).

3. Data analysis

Experimental data were recorded and analyzed using Microsoft Excel 2019 for statistical processing, and graphs were plotted using Origin 2021 software. All experiments were performed in triplicate, and the results are expressed as mean ± standard deviation.

4. Results and discussions

4.1.Encapsulation efficiency and optimization of process conditions

Encapsulation efficiency (EE) serves as a critical metric for evaluating the performance of encapsulation systems, as it quantitatively reflects the retention capacity of active components during the encapsulation process (Li et al., 2018). In the preparation of microcapsules and related products, EE represents a fundamental quality parameter. To determine the EE of gingerol microcapsules, the quantification of total oil and surface oil content was initially conducted. The encapsulation efficiency was subsequently calculated using the standard formula for EE determination.

The optimization of operational conditions was systematically investigated through a single-factor experimental approach, establishing the following optimal parameters: a wall-to-core material ratio of 5:1, a solid content of 10%, an Arabic gum concentration of 55% in the wall material, and an emulsifier content of 1%. A comprehensive experimental design comprising 29 distinct combinations was implemented, with the corresponding results presented in Table 2. The experimental data revealed that the maximum EE of 71.74% was achieved in experiment 19, while the minimum EE of 54.71% was observed in experiment 14. The experimental EE data were subjected to rigorous regression analysis using Design-Expert software, yielding the following polynomial regression model equation:

$$EE\ (\%) = 70.88 + 0.6592A - 1.76B + 0.8108C + 0.4483D - 2.03AB - 1.67AC + 0.095AD + 3.25BC + 1.39BD - 0.63CD - 5.4A^2 - 4.52B^2 - 5.05C^2 - 4.18D^2 \quad (6)$$

where A, B, C, and D represent the coded values of the independent variables in the experimental design. This model provides a quantitative framework for predicting and optimizing encapsulation efficiency under various process conditions.

Table 2. Experimental design matrix and corresponding response surface methodology (RSM) results

Number	Coded variables				EE (%)
	A	B	C	D	
1	0	0	1	1	61.08
2	-1	0	0	-1	59.58
3	0	-1	0	-1	64.78
4	-1	-1	0	0	60.45
5	0	1	1	0	64.40
6	0	-1	-1	0	64.91
7	1	0	0	1	63.41
8	-1	1	0	0	60.20
9	1	0	-1	0	62.81
10	1	1	0	0	56.82
11	-1	0	1	0	61.82
12	0	1	0	-1	59.46
13	1	0	1	0	60.25
14	0	1	-1	0	54.71

15	0	0	-1	-1	60.38
16	1	-1	0	0	65.20
17	0	0	0	0	70.85
18	0	0	1	-1	62.53
19	0	0	0	0	71.74
20	1	0	0	-1	60.88
21	0	0	-1	1	61.45
22	0	-1	1	0	61.59
23	0	0	0	0	70.41
24	0	0	0	0	69.69
25	-1	0	-1	0	57.68
26	-1	0	0	1	61.73
27	0	1	0	1	62.78
28	0	-1	0	1	62.54
29	0	0	0	0	71.72

Table 3. Analysis of variance and statistical parameters of the model

Source	**SS[a]**	**DF[b]**	**MS[c]**	***F*- value**	***p* -Value**	**Significance[d]**
Model	518.24	14	37.02	38.34	< 0.0001	**
A	5.21	1	5.21	5.40	0.0357	*
B	37.10	1	37.10	38.43	< 0.0001	**
C	7.89	1	7.89	8.17	0.0126	*
D	2.41	1	2.41	2.50	0.1363	
AB	16.52	1	16.52	17.11	0.0010	**
AC	11.22	1	11.22	11.62	0.0042	**
AD	0.0361	1	0.0361	0.0374	0.8495	
BC	42.32	1	42.32	43.83	< 0.0001	**
BD	7.73	1	7.73	8.00	0.0134	*
CD	1.59	1	1.59	1.64	0.2206	
A^2	188.95	1	188.95	195.70	< 0.0001	**
B^2	132.58	1	132.58	137.32	< 0.0001	**
C^2	165.41	1	165.41	171.32	< 0.0001	**
D^2	113.12	1	113.12	117.16	< 0.0001	**
Residual	13.52	14	0.9655			
Lack of Fit	10.43	10	1.04	1.35	0.4134	
Pure Error	3.08	4	0.7708			
Cor Total	531.76	28				

R^2=0.9746; R^2_{Adj}=0.9492

[a] SS= sum of squares; [b] DF =degree of freedom; [c] MS = mean square; [d] significance: * $p < 0.05$ is significant.

The validity and significance of the regression equation were rigorously evaluated through analysis of variance (ANOVA). As demonstrated in Table 3, the regression model exhibited excellent predictive capability, with a coefficient of determination (R^2) of 0.9746 and

an adjusted R^2 (R^2_{Adj}) of 0.9492. The model's statistical significance was confirmed by a p-value < 0.0001, indicating a highly reliable mathematical relationship between the independent variables and encapsulation efficiency.

Response Surface Methodology (RSM) analysis revealed that solid content (B) exerted the most substantial influence on the encapsulation efficiency of gingerol microcapsules ($p < 0.01$). Subsequent analysis identified the wall-to-core ratio (A) and Arabic gum content in the wall material (C) as additional significant factors affecting encapsulation efficiency ($p < 0.05$). These findings can be mechanistically explained by the fundamental role of solid content in microcapsule formation dynamics.

During microencapsulation, insufficient solid content may lead to inadequate dispersion of gingerol within the wall matrix, resulting in elevated levels of free gingerol. Furthermore, low solid content compromises the integrity of the wall film formation, yielding an unstable membrane architecture (Fernandes et al., 2017). This structural instability subsequently impedes the generation of uniform particles during spray drying, increasing microcapsule fragility and ultimately diminishing encapsulation efficiency.

Conversely, excessive solid content presents alternative challenges. The inherent adhesive properties of solid materials such as Arabic gum and whey protein can induce excessive viscosity in the emulsion system when present at elevated concentrations. This heightened viscosity hinders the homogeneous dispersion of gingerol, promoting molecular aggregation and resulting in non-uniform encapsulation, thereby negatively impacting encapsulation efficiency (Wangkulangkool et al., 2023).

The wall-to-core ratio represents another critical parameter influencing encapsulation performance. Insufficient wall material compromises the encapsulation capacity, exposing gingerol to environmental stressors such as oxidation, photodegradation, and thermal fluctuations, ultimately leading to active ingredient degradation and reduced encapsulation efficiency. Conversely, excessive wall material, while enhancing protective capacity, may result in overly dense microcapsule structures. This structural compaction can impede the uniform distribution of gingerol within the wall matrix, potentially leading to void formation and subsequent reduction in encapsulation efficiency (San et al., 2022).

The compositional ratio of Arabic gum to whey protein in the wall material significantly impacts encapsulation efficiency, a phenomenon attributable to the distinct physicochemical properties of these biopolymers. Variations in the Arabic gum: whey protein ratio directly modulate the physical architecture of the composite wall matrix. The pronounced hydrophilicity of Arabic gum facilitates gingerol dispersion within the aqueous phase, promoting uniform distribution within the wall material. However, disproportionate increases in Arabic gum content may result in excessive membrane porosity and colloidal instability, potentially compromising gingerol retention and reducing encapsulation efficiency.

In contrast, whey protein demonstrates exceptional emulsification properties, which facilitate the homogeneous dispersion of gingerol within the wall matrix, particularly in oil/water emulsion systems. However, the pronounced gelation characteristics of whey protein can induce excessive rigidity and density in the wall material when present at elevated concentrations, thereby compromising gingerol dispersibility and reducing encapsulation efficiency. Consequently, optimization of the Arabic gum-to-whey protein ratio is crucial for achieving efficient gingerol encapsulation, preventing active compound loss, and enhancing its stability and bioavailability in subsequent applications (Ahad et al., 2021).

RSM analysis further revealed that among the quadratic and interaction terms of the independent variables, the BD interaction term exhibited statistical significance ($p < 0.05$), while the AC, BC interactions, and all

quadratic terms demonstrated highly significant effects ($p < 0.01$). These findings indicate that the relationship between experimental factors and the response variable is characterized by complex non-linear interactions rather than simple linear correlations.

Based on these insights, the experimental parameters were further optimized using Design-Expert software, yielding the following optimal process conditions: a wall-to-core ratio of 5.103:1 (w/w), a solid content of 8.912% (wt%), an Arabic gum content of 54.916% (wt%), and an emulsifier content of 1.019% (wt%). Under these optimized conditions, the predicted encapsulation efficiency of gingerol microcapsules reached 71.11%. Experimental validation through triplicate trials yielded an average encapsulation efficiency of 71.83%, demonstrating minimal deviation (0.72%) from the theoretical prediction. This close agreement between experimental and predicted values validates the model's reliability and confirms its predictive accuracy for determining the actual encapsulation efficiency of microcapsules.

4.2. Analysis of microcapsule physical characteristics

The process-optimized microencapsulated gingerol demonstrated an encapsulation yield of 91.18% ± 1.34% (Table 4), quantitatively representing the efficiency of the microencapsulation process and the quality of the final product. This exceptionally high yield confirms the successful retention and encapsulation of gingerol within the microcapsule matrix.

Moisture content, a critical quality attribute for food stability and safety, was determined to be 2.66% ± 0.33% for the optimized microcapsules. Such low hygroscopicity aligns with stringent microcapsule specifications and effectively mitigates microbial proliferation risks during storage (Zhang et al., 2022).

Solubility analysis revealed a dissolution capacity of 94.58% ± 0.54% for the gingerol microcapsules (Table 4). This superior performance stems from the synergistic interplay of the GA-whey protein binary composite matrix. Compared to single-component wall materials, the GA/WPI hybrid system demonstrates enhanced modulation of gingerol dissolution kinetics (Zhang et al., 2022).

The hydrophilic domains of GA facilitate rapid hydration, while the gel-forming propensity of WPI governs controlled release dynamics. This dual-phase behavior optimizes gingerol bioavailability by balancing dissolution efficiency with sustained release characteristics.

Table 4. Physical properties of spray-dried gingerol microcapsules

Parameters	Gingerol Microcapsules
Powder yield (%)	91.18±1.34
Solubility (%)	94.58±0.54
Moisture content (%)	2.66±0.33
Moment Integral (MI, nm)	391.67±3.75
$D_{(90)}$ (nm)	761.33±9.11
$D_{(50)}$ (nm)	322.67±2.34
Size distribution, PDI	0.37±0.02
Zeta potential (mV)	-23.6±0.35

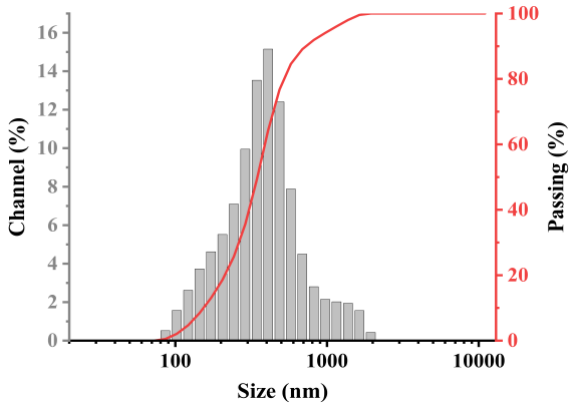

Figure 1. Particle size distribution of gingerol microcapsules

Particle size, size distribution, zeta potential (ζ-potential), and polydispersity index (PDI) serve as critical parameters for assessing the physical attributes, colloidal stability, and functional performance of particulate systems. The particle size of microcapsules, expressed as the volumetric mean diameter (D_{50}), is a fundamental determinant of encapsulation efficiency, payload capacity, structural integrity, and controlled-release kinetics of bioactive compounds (Wang et al., 2021). Size distribution quantifies dimensional heterogeneity within the population, while PDI numerically characterizes the breadth of this distribution, with lower values (PDI < 0.4) indicating superior monodispersity (Fernandes et al., 2017).

As evidenced by the data in Table 4 and the size distribution profile (Figure 1), the optimized gingerol-loaded microcapsules exhibited a mean particle size (D_{50}) of 322.67 nm, with 90% of the population (D_{90}) below 761.33 nm. The PDI of 0.37 (< 0.4 threshold) confirms a narrow size distribution and high uniformity across the particle population. Notably, the volumetric mean diameter (391.67 nm) reflects a predominantly submicron particle distribution, with a minor fraction exceeding 760 nm.

The ζ-potential measurement of -23.6 mV (absolute value > 20 mV) indicates robust colloidal stability, where electrostatic repulsion between particles effectively counterbalances van der Waals attractive forces, thereby preventing aggregation and sedimentation (Nami et al., 2023). This stability profile, combined with the observed monodispersity, positions these microcapsules as promising candidates for controlled-release applications.

Collectively, the optimized microcapsules demonstrate:

1. Controlled size distribution: Narrow PDI (0.37) ensures batch-to-batch reproducibility and predictable release kinetics.
2. Enhanced stability: High ζ-potential magnitude (-23.6 mV) confers long-term colloidal stability.
3. Functional superiority: Submicron-scale dimensions (D_{50}: 322.67 nm) optimize surface-to-volume ratios for efficient bioactive delivery.

These findings underscore the formulation's potential for advanced drug delivery systems, where precise control over physicochemical properties directly translates to enhanced therapeutic efficacy and shelf-life stability.

4.3. Fourier transform infrared spectroscopy (FTIR) analysis

As illustrated in the FTIR spectra (Figure 2), the whey protein isolate (WPI) exhibits characteristic absorption bands at 2960 cm^{-1} and 2925 cm^{-1}, which were attributed to asymmetric C-H stretching vibrations in methyl ($-CH_3$) and methylene ($-CH_2$) groups, respectively (Zhang et al., 2022). These vibrations primarily originate from aliphatic chains in fatty acids and hydrophobic amino

acid residues within the protein matrix. Two prominent absorption bands at 1656 cm^{-1} and 1542 cm^{-1} were also observed, corresponding to amide I (C=O stretching) and amide II (N-H bending coupled with C-N stretching) vibrations, indicative of protein secondary structures.

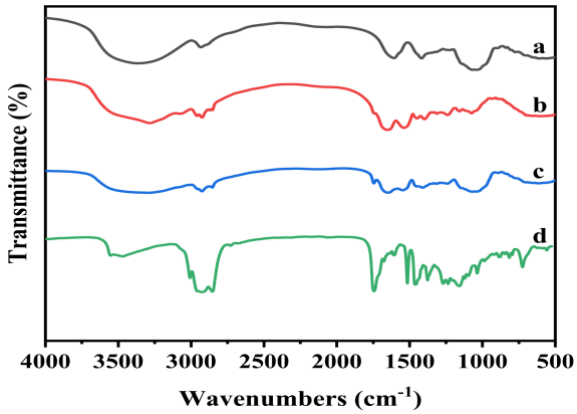

Figure 2. FTIR spectra of GA (a), WPI(b), microcapsules (c), and gingerol crude oil (d)

In the gum arabic (GA) spectrum, characteristic polysaccharide absorption bands were identified at 2933 cm^{-1} (-CH stretching) and 1070 cm^{-1} (-C-O-C stretching), consistent with its carbohydrate backbone (Nguyen et al., 2024). The gingerol spectrum displayed distinct peaks at 1605 cm^{-1} (C=C aromatic ring stretching), 1745 cm^{-1} (carbonyl group, C=O stretching), and 2854–2924 cm^{-1} (C-H stretching of aromatic and alkene groups) (Mohammadi et al., 2023).

The FTIR spectrum of the microcapsules largely mirrored the spectral profiles of the wall materials (GA and WPI), though notable intensity reductions and peak shifts were detected. Specifically, the diminished intensity at 2854 cm^{-1} (-CH vibrations) and a slight shift at 2924 cm^{-1} suggested molecular interactions between the -CH groups of WPI, GA, and encapsulated gingerol. Furthermore, the weakening of the carbonyl stretching band at 1745 cm^{-1} in gingerol microcapsules may be ascribed to hydrogen bonding between the amide group (–CONH) of WPI, carboxyl groups (–COOH) of GA, and hydroxyl moieties in gingerol. Crucially, no new absorption bands were detected in the microcapsule spectrum, confirming the absence of covalent bond formation during encapsulation. These spectral modifications collectively validate the successful physical entrapment of gingerol within the GA-WPI matrix while preserving its native chemical structure (Tahir et al., 2024).

4.4. X-ray diffraction (XRD) analysis

X-ray diffraction (XRD) was employed to investigate the crystallographic properties, including phase composition, crystallite size, and lattice structure of the materials. The technique operates on the principle of X-ray interaction with crystalline lattices, wherein atomic planes induce diffraction patterns. By analyzing diffraction angles (2θ) and intensity profiles (I), structural information such as lattice parameters and phase purity can be derived. While XRD is conventionally applied to crystalline systems, it also provides insights into amorphous materials, which typically manifest as broad scattering halos in diffraction spectra.

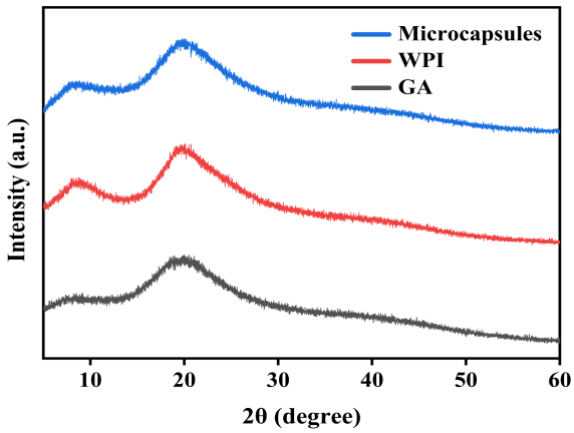

Figure 3. X-ray diffraction patterns of GA, WPI, and microcapsules

The XRD patterns of all samples (Figure 3) displayed characteristic broad and diffuse scattering halos, confirming their amorphous nature. This similarity suggests that the microencapsulation process, including the elevated temperatures associated with spray drying, did not induce crystallization or alter the inherent material properties, preserving the amorphous state throughout processing. Among the samples, gum arabic (GA) exhibited the weakest diffraction intensity, consistent with its disordered polysaccharide structure. In contrast, whey protein isolate (WPI) demonstrated marginally sharper diffraction features, likely attributable to its partially ordered molecular arrangement, which may include microcrystalline domains or regions of localized structural regularity (Ahad et al., 2023). These observations imply that WPI contributes more significantly to the structural integrity of the microencapsulation system compared to GA.

4.5. Scanning electron microscopy analysis

As shown in the SEM micrographs (Figure 4), the spray-dried gingerol microcapsules exhibited spherical morphology with smooth surfaces and polydisperse size distribution. The particles were largely devoid of macroscopic defects such as fractures or visible pores, indicating effective encapsulation of gingerol by the gum arabic (GA) and whey protein isolate (WPI) composite matrix, which likely enhanced core material protection (Wangkulangkool et al., 2023).

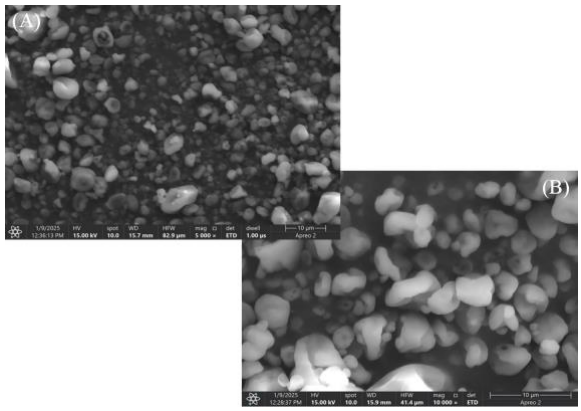

Figure 4. SEM images of gingerol microcapsules at magnifications of 5000× (A) and 10000× (B)

A prominent feature observed in the majority of microcapsules was the presence of surface wrinkles and concavities, likely attributable to rapid water evaporation and subsequent matrix contraction during the drying process. Additionally, localized surface irregularities, including micropores and textured domains, were identified. These

features may arise from the film-forming characteristics of GA, which typically produces semipermeable matrices with inherent microporosity. The synergistic interaction between GA and WPI during film formation further modulated the surface topography, potentially amplifying these structural heterogeneities. Such morphological attributes, particularly the microporous architecture, are hypothesized to play a critical role in governing the diffusion kinetics of encapsulated compounds, suggesting functional implications for modulating controlled release kinetics (Ahad et al., 2022).

4.6. Storage stability

The comparative stability profiles of unencapsulated gingerol and gingerol microcapsules under distinct storage conditions are summarized in Figure 5. Both systems exhibited time-dependent reductions in retention rates over the 12-day study period, though the microencapsulated form demonstrated superior stability across all tested conditions. This observation underscores the protective efficacy of the gum arabic (GA) and whey protein isolate (WPI) composite wall matrix in preserving gingerol integrity.

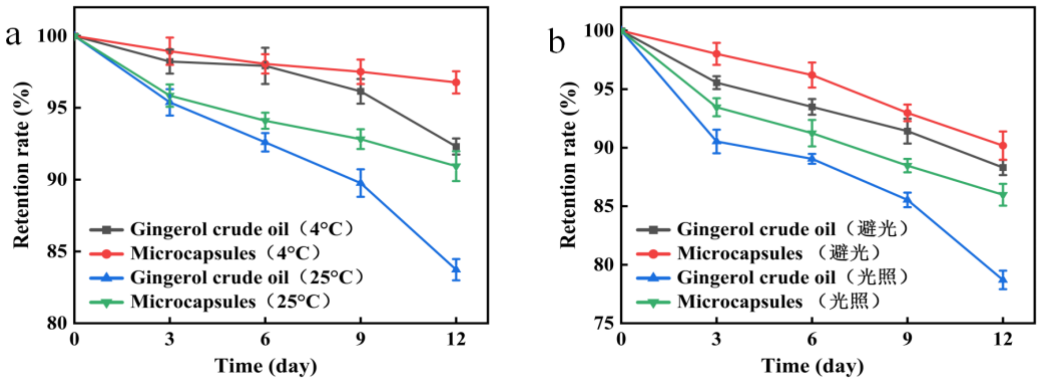

Figure 5. Retention rate of gingerol content in microcapsules and gingerol crude oil under different storage conditions: (a) 4°C and 25°C; (b) natural light and dark conditions

At 4°C, retention rates for unencapsulated gingerol and microcapsules remained above 90% after 12 days, confirming enhanced stability under refrigeration. At ambient temperature (25°C), microcapsules retained 90.94% of initial gingerol content, significantly exceeding the 83.73% retention observed for the unencapsulated form. These results highlight the temperature-sensitive degradation kinetics of gingerol, with microencapsulation substantially mitigating thermal degradation.

Light exposure markedly accelerated gingerol degradation, as evidenced by retention rates of 78.70% (free gingerol) and 85.98% (microcapsules) after 12 days under illumination. In contrast, dark-stored counterparts exhibited retention rates of 88.31% and 90.18%, respectively, emphasizing gingerol's inherent photosensitivity. The structural vulnerability arises from its polyphenolic nature, where hydroxyl groups facilitate oxidative degradation via light-induced radical formation. Additionally, UV radiation may induce photolytic cleavage of alkene double bonds in gingerol's aliphatic chain, further exacerbating degradation.

Notably, the microcapsules' higher retention under light stress demonstrates their photoprotective efficacy, likely mediated by the GA-WPI matrix acting as a light-scattering barrier and antioxidant reservoir. These findings collectively validate microencapsulation as an effective strategy to enhance gingerol's environmental stability while preserving its bioactive properties.

4.7. Antioxidant activity evaluation

4.7.1 DPPH Radical Scavenging Activity of Microcapsules

The DPPH (2,2-diphenyl-1-picrylhydrazyl) radical scavenging assay evaluates antioxidant capacity through the reduction of the stable nitrogen-centered DPPH radical (purple) to its non-radical form (DPPH-H, colorless) via hydrogen donation. This scavenging activity is strongly correlated with phenolic content, such as gingerol, and exhibits concentration-dependent behavior.

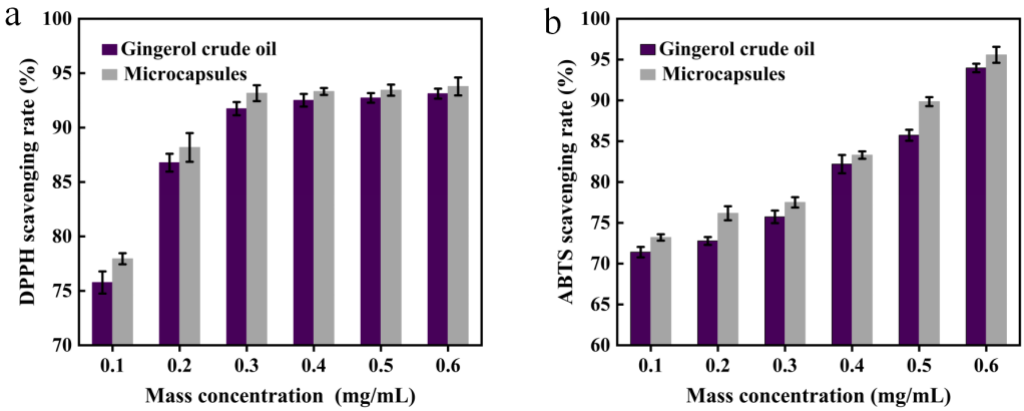

Figure 6. Antioxidant activity of microcapsules and gingerol crude oil: (a) DPPH radical scavenging activity; (b) ABTS radical scavenging activity

As shown in Figure 6A, both free gingerol and microencapsulated gingerol demonstrated dose-dependent increases in DPPH radical scavenging activity, with no statistically significant differences ($p > 0.05$) between the two forms. However, the microcapsules exhibited marginally higher scavenging rates at equivalent concentrations. For example, at 0.1 mg/mL gingerol, scavenging rates reached 77.95% (microcapsules) versus 75.77% (free gingerol). This enhancement is attributed to gingerol's intrinsic antioxidant potency, as gum arabic (GA) and whey protein isolate (WPI) possess only weak radical-neutralizing capabilities relative to the core compound.

Notably, prior studies corroborate the compatibility of GA and WPI in antioxidant systems. Xu et al. (2019) reported that chitosan-GA composite films exhibited elevated antioxidant activity with increasing GA ratios (1:0 to 1:2), suggesting GA's auxiliary role in stabilizing phenolic compounds. Similarly, Chiang et al. (2020) documented WPI's DPPH scavenging rates of 42.3–86.8% at 20 mg/mL, confirming its non-interfering yet contributory antioxidant behavior. These findings align with the current results, implying that GA and WPI neither impede gingerol's radical scavenging activity nor act as competitive inhibitors. Instead, the wall materials may synergistically enhance gingerol's stability and bioavailability, thereby amplifying its functional efficacy.

4.7.2 ABTS Radical Scavenging Activity of Microcapsules

The $ABTS^+$ radical scavenging assay involves the generation of a stable cationic radical ($ABTS^+$) through oxidation of ABTS (2,2′-azino-bis(3-ethylbenzothiazoline-6-sulfonic acid)) with oxidizing agents such as potassium persulfate or hydrogen peroxide, yielding a characteristic blue-green chromophore. Antioxidant activity is quantified by the reduction of $ABTS^+$ to its non-radical form, accompanied by a proportional decrease in absorbance at 734 nm.

As illustrated in Figure 6B, both free gingerol and gingerol microcapsules exhibited concentration-dependent $ABTS^+$ scavenging activity within the tested range (0.1–0.6 mg/mL). Notably, even at low concentrations (<0.3 mg/mL), both systems demonstrated substantial radical neutralization (>65%), underscoring gingerol's intrinsic antioxidant

potency. Microencapsulation further enhanced scavenging efficiency, with encapsulated gingerol achieving marginally higher activity than its unencapsulated counterpart. This improvement may arise from synergistic interactions between gingerol and the wall materials, gum arabic (GA) and whey protein isolate (WPI), which possess mild antioxidant properties and contribute to oxidative stabilization.

The observed enhancement aligns with prior studies on bioactive encapsulation. Hu et al. (2018) reported that GA-WPI composites improved the oxidative stability of flavonoids by forming protective interfacial layers in emulsions, thereby mitigating degradation and amplifying radical scavenging capacity. Similarly, the GA-WPI matrix in this study likely acts as a physical barrier, reducing gingerol's exposure to pro-oxidative environments while facilitating synergistic electron transfer between the core and wall materials. These mechanisms collectively enhance the microcapsules' antioxidant performance without compromising gingerol's bioactivity.

4.8. Preservation of beef

4.8.1 pH Value

The pH value of meat serves as a critical biochemical indicator for assessing quality, freshness, and safety, with its fluctuations closely linked to myoglobin oxidation and microbial metabolic activity during storage (Jia et al., 2021). As illustrated in Figure 7, the pH profiles of all treatment groups exhibited a biphasic trend: initial decline followed by gradual increase over the storage period, mirroring oxidative color changes in beef.

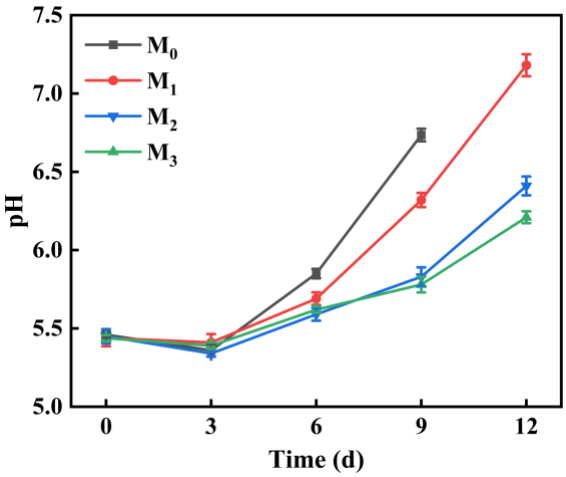

Figure 7. Changes in pH values of beef samples from different treatment groups over time during cold storage. Treatment groups: M_0 (blank control), M_1 (empty capsule), M_2 (gingerol crude oil), M_3 (microcapsules)

During the initial 0–3 days, post-mortem anaerobic glycolysis in muscle tissue generated lactic acid accumulation, driving pH reduction across all groups (Yang et al., 2023). This phase coincided with transient brightening of beef coloration due to deoxymyoglobin formation. Between days 3–6, pH values rebounded progressively, correlating with the onset of surface darkening caused by metmyoglobin accumulation. This reversal reflects the metabolic dominance of psychrotrophic spoilage microbiota, whose alkaline metabolites (e.g., ammonia, trimethylamine) and proteolytic activity counteracted lactic acidification. Notably, low-temperature refrigeration attenuated microbial growth kinetics, moderating pH escalation rates.

Post-day 6, divergent pH trajectories emerged among treatments. The control group (M_0) displayed the steepest pH increase (reaching spoilage threshold pH > 6.7 by day 9), paralleling rapid chromatic degradation to brown hues. In contrast, gingerol-containing groups (M_2, M_3) exhibited suppressed pH

elevation, with M_3 demonstrating the most stable profile due to microencapsulation-enhanced retention of antimicrobial efficacy. By day 12, M_1 (gingerol-free) reached full spoilage (pH 6.8), while M_2 and M_3 maintained pH values below 6.5, confirming gingerol's capacity to inhibit spoilage-associated alkalization.

These findings demonstrate that gingerol disrupts microbial decarboxylase activity and protein degradation pathways, thereby stabilizing pH within freshness thresholds. Microencapsulation technology further prolongs this effect through controlled-release kinetics, delaying spoilage-induced pH shifts by 3–6 days compared to unprotected samples. The strong correlation between pH dynamics, microbial proliferation, and oxidative color changes underscores pH's utility as a multifunctional freshness marker in meat preservation systems.

4.8.2 Aerobic plate count (APC)

Microbial proliferation represents the primary mechanism of spoilage in meat products, with aerobic plate count (APC) serving as a standard microbiological metric to evaluate spoilage progression and hygienic quality (Cheng et al., 2021).

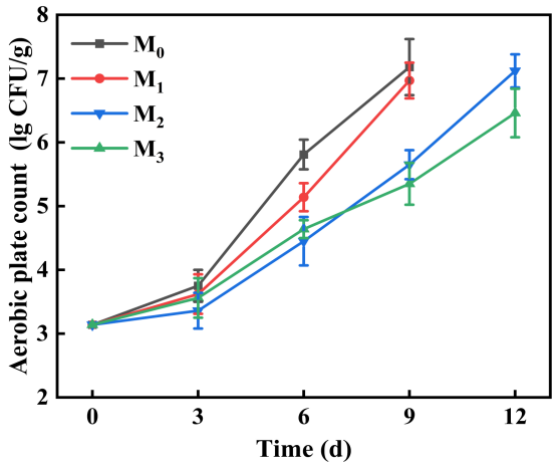

Figure 8. Changes in aerobic plate count (APC) of beef samples from different treatment groups over time during cold storage. Data represent mean lg CFU/g ± standard deviation (n = 3)

Figure 8 illustrates the temporal evolution of APC values across experimental groups during storage. The initial APC of fresh beef was quantified at 3.14lg CFU/g, consistent with typical baseline microbial loads in unprocessed meat. Progressive increases in APC were observed in both control (M_0) and treatment groups, though divergence in microbial growth kinetics emerged during storage. Notably, the M_0 group exhibited accelerated APC accumulation relative to other treatments, correlating with macroscopic color degradation from bright red to darkened brown or dark red hues. Such color changes serve as a visual indicator of advanced spoilage, which is associated with the production of microbial metabolites and myoglobin oxidation. (Li et al., 2024). This chromatic shift was most pronounced in M_0, aligning with its elevated APC trajectory.

By day 6, the M_0 group approached the established spoilage threshold for meat products (6.0lg CFU/g) with an APC of 5.81lg CFU/g. In contrast, the M_1 group demonstrated moderated microbial growth (reduced APC values), likely attributable to partial antimicrobial activity conferred by the microencapsulation-derived surface film acting as a physical barrier against contamination. By day 9, both M_0 (7.18lg CFU/g) and M_1 (6.97lg CFU/g) exceeded critical spoilage limits, confirming product deterioration. Conversely, M_2 and M_3 groups maintained APC levels below 6.0lg CFU/g through day 8, demonstrating gingerol's dose-dependent antimicrobial efficacy in delaying spoilage.

Comparative analysis of M_2 and M_3 groups revealed distinct kinetic profiles: M_3 exhibited attenuated APC growth post-day 6, reflecting time-dependent cumulative release of gingerol from microcapsules. Early-stage release kinetics in M_3 likely delivered sub-inhibitory concentrations, whereas M_2's immediate availability of free gingerol provided more rapid antimicrobial action. However, sustained release from microcapsules in M_3 ultimately enhanced prolonged suppression of microbial proliferation, as evidenced by reduced APC growth rates relative to M_2 after day 6 (Brilliana et al., 2017). Both treatment groups reached spoilage thresholds by day 12, indicating that microencapsulated gingerol extended beef shelf life by 3–4 days compared to controls.

4.8.3 Total volatile basic nitrogen (TVB-N)

Total Volatile Basic Nitrogen (TVB-N), a collective measure of ammonia (NH_3) and volatile amines (e.g., methylamine, ethylamine), is generated through microbial and enzymatic proteolysis during meat spoilage. This parameter serves as a critical biochemical indicator of protein degradation and freshness decline in meat products (Kyrana et al., 1997). Figure 9 depicts the temporal progression of TVB-N values across experimental groups during storage. All groups exhibited incremental TVB-N increases over time, consistent with aerobic plate count (APC) trends (Cao et al., 2022). According to the Chinese national standard GB 2707-2016, fresh meat must maintain TVB-N levels below 15 mg/100 g. Values exceeding this threshold are indicative of advanced spoilage.

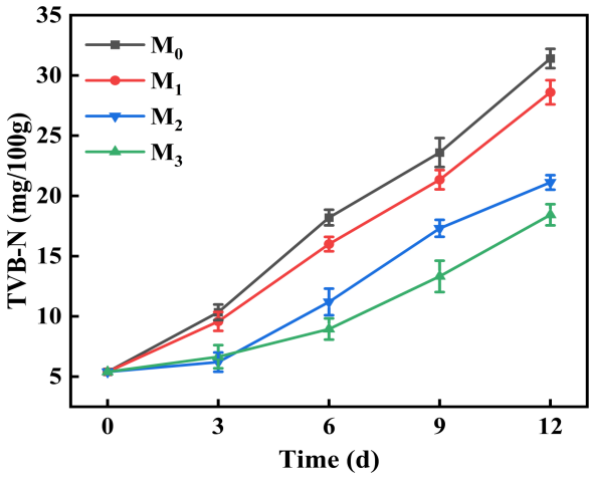

Figure 9. Changes in TVB-N values of beef samples from different treatment groups over time during refrigerated storage

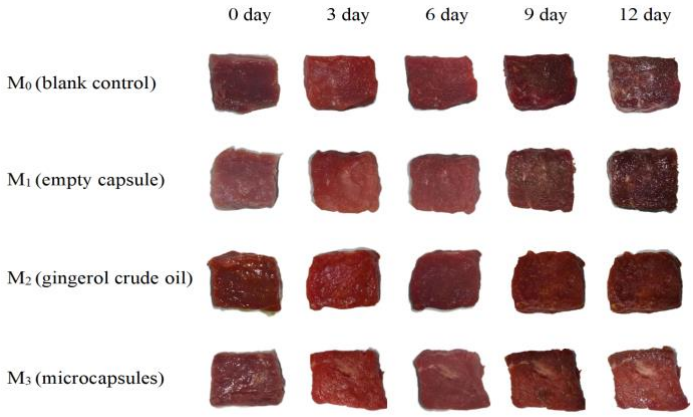

Figure 10. Changes in texture and color attributes of beef samples from different treatment groups over time during refrigerated storage

During the initial 3 days of storage, all groups retained TVB-N values within the freshness limit (<15 mg/100 g). By day 6, however, the control (M_0) and M_1 groups surpassed the spoilage threshold, concomitant with pronounced chromatic shifts toward brown discoloration (a visual manifestation of heme protein oxidation and proteolytic metabolite accumulation). In contrast, M_2 and M_3 groups maintained significantly lower TVB-N levels ($p<0.05$) and delayed color degradation, demonstrating gingerol's capacity to suppress microbial proliferation and proteolytic activity(Figure.10).

Comparative analysis revealed distinct spoilage kinetics: M_1 exhibited marginally reduced TVB-N values relative to M_0, whereas M_2 and M_3 exceeded the regulatory limit on days 9 (17.31 mg/100 g) and 12 (18.43 mg/100 g), respectively. This divergence highlights the microencapsulation system's dual functionality: (1) formation of a semi-permeable surface barrier limiting oxidative processes and microbial colonization, and (2) sustained release of gingerol to inhibit spoilage-associated enzymatic pathways. Notably, M_3 displayed attenuated TVB-N escalation after day 3, attributable to time-dependent release kinetics of microencapsulated gingerol that prolonged antimicrobial efficacy (Qiu et al., 2022). These findings confirm that microencapsulation technology enhances gingerol's preservative action, extending beef shelf life by 3–6 days compared to unprotected samples.

5. Conclusions

This study employed gum arabic (GA) and whey protein isolate (WPI) as composite wall materials to fabricate gingerol-loaded microcapsules via spray drying, with process parameters optimized using a response surface methodology (RSM) model. The optimal microencapsulation conditions were identified as follows: wall-to-core material ratio (5.103:1, w/w), solid content (8.912%, w/w), GA proportion (54.916%, w/w), and emulsifier concentration (1.019%, w/w). Under these RSM-optimized conditions, the gingerol encapsulation efficiency reached 71.83%. The resultant microcapsules exhibited favorable physicochemical properties, including stable ζ-potential (-23.6 mV) and high aqueous solubility (94.58%). Comparative evaluation revealed that encapsulated gingerol demonstrated enhanced antimicrobial and antioxidant activities under refrigerated conditions relative to its free form. Application studies on beef preservation demonstrated that the microcapsules effectively suppressed microbial proliferation and lipid oxidation on meat surfaces. Furthermore, the encapsulation conferred sustained protection, enabling prolonged bioactive efficacy of gingerol during low-temperature storage, thereby extending the shelf life of fresh beef by 3-4 days. These findings validate the preservative potential of gingerol microcapsules, which exhibited improved stability, solubility, and reduced environmental sensitivity compared to unencapsulated counterparts. The successful implementation of gingerol microencapsulation in fresh beef preservation establishes a methodological framework for potential applications in other perishable food systems.

6. References

Ahad, T., Gull, A., Masoodi, F.A., Gani, A., Nissar, J., Ganaie, T.A., (2023). Masoodi, L. Protein and polysaccharide based encapsulation of ginger oleoresin: impact of wall materials on powder stability, release rate and antimicrobial characteristics. *International Journal of Biological Macromolecules*, 240, 124331.

Ahad, T., Gull, A., Masoodi, F.A., Hussein, D.S., Alkahtani, J. (2024). Effect of process parameters on production of ginger oleoresin powder by spray drying using whey protein isolate as the wall material. *Biomass Conversion and Biorefinery*, 14(21), 27735-27744.

Ahad, T., Gull, A., Masoodi, F.A., Nissar, J., Masoodi, L., Sajad Wani, M. (2023). Effect of excipient wall materials on the development of ginger oleoresin microcapsules: assessing the physicochemical, antioxidant and structural

properties. *Journal of the Science of Food and Agriculture*, 103(1), 73-82.

Ahad, T., Masoodi, F.A., Gull, A., Wani, S.M., Shafi, M.N. (2021). Optimization of process parameters for spray drying of ginger oleoresin powder using response surface methodology. *Journal of food processing and preservation*, 45(4), e15190.

Al-Hamayda, A., Abu-Jdayil, B., Ayash, M., Tannous, J. (2023). Advances in microencapsulation techniques using Arabic gum: A comprehensive review. *Industrial Crops and Products*, 205, 117556.

Brilliana, I.N., Manuhara, G.J., Utami, R., Khasanah, L.U. (2017). The effect of cinnamon bark (Cinnamomum burmanii) essential oil microcapsules on vacuumed ground beef quality. *IOP Conference Series: Materials Science and Engineering*, 193(1), 012057.

Cao, Y., Hao, R., Guo, Z., Han, L., Yu, Q., Zhang, W. (2022). Combined effects of superchilling and natural extracts on beef preservation quality. *Lwt*, 153, 112520.

Chen, P., Yang, Q., Zhang, L., Zhong, R., Cao, Y., Miao, J. (2024). Ginger Essential Oil Extracted by Low-Temperature Continuous Phase Transition and Its Preservation Effect on Prepared Duck Meat. *Food and Bioprocess Technology*, 18(3), 2806-2819.

Cheng, Y., Hu, J., Wu, S. (2021). Chitosan based coatings extend the shelf-life of beef slices during refrigerated storage. *Lwt*, 138, 110694.

Chiang, S.H., Chang, C.Y. (2020). Antioxidant properties of caseins and whey proteins from colostrums. *Journal of Food and Drug Analysis*, 13(1), 6.

Devi, L.M., Das, A.B., Badwaik, L.S. (2023). Effect of gelatin and acacia gum on anthocyanin coacervated microcapsules using double emulsion and its characterization. *International Journal of Biological Macromolecules*, 235, 123896.

Fernandes, R.V.D.B., Botrel, D.A., Silva, E.K., Pereira, C.G., Carmo, E.L.D., Dessimoni, A.L.D.A., Borges, S.V. (2017). Microencapsulated ginger oil properties: Influence of operating parameters. *Drying Technology*, 35(9), 1098-1107.

Fernandes, R.V.D.B., Silva, E.K., Borges, S.V., de Oliveira, C.R., Yoshida, M.I., da Silva, Y.F., Botrel, D.A. (2017). Proposing Novel Encapsulating Matrices for Spray-Dried Ginger Essential Oil from the Whey Protein Isolate-Inulin/Maltodextrin Blends. *Food and Bioprocess Technology*, 10(1), 115-130.

Ghasemzadeh, A., Jaafar, H.Z.E., Baghdadi, A., Tayebi-Meigooni, A. (2018). Formation of 6-, 8- and 10-Shogaol in Ginger through Application of Different Drying Methods: Altered Antioxidant and Antimicrobial Activity. *Molecules*, 23(7), 1646.

Hu, Y., Li, Y., Zhang, W., Kou, G., Zhou, Z. (2018). Physical stability and antioxidant activity of citrus flavonoids in arabic gum-stabilized microcapsules: Modulation of whey protein concentrate. *Food Hydrocolloids*, 77, 588-597.

Huang, J., Chen, Q., Qiu, M., Li, S. (2012). Chitosan-based Edible Coatings for Quality Preservation of Postharvest Whiteleg Shrimp (Litopenaeus vannamei). *Journal of Food Science*, 77(4), C491-C496.

Ivane, N.M.A., Elyse, F.K.R., Haruna, S.A., Pride, N., Richard, E., Foncha, A.C., Dandago, M.A. (2022). The anti-oxidative potential of ginger extract and its constituent on meat protein isolate under induced Fenton oxidation. *Journal of Proteomics*, 269, 104723.

Jia, R., Ge, S., Ren, S., Luo, Y., Xiu, L., Sanabil, Liu, H., Cai, D. (2021). Antibacterial mechanism of adzuki bean seed coat polyphenols and their potential application in preservation of fresh raw beef. *International Journal of Food Science & Technology*, 56(10), 5025-5039.

Kalajahi, S..G, Malekjani, N., Samborska, K., Akbarbaglu, Z., Gharehbeglou, P., Sarabandi, K., Jafari, S.M. (2023). The enzymatic modification of whey-proteins for spray drying encapsulation of Ginkgo-biloba extract. *International Journal of Biological Macromolecules*, 245, 125548.

Kamaruddin, M.S.H., Chong, G.H,. Daud, N.M., Putra, N.R., Salleh, L.M. (2023).

Suleiman N. Bioactivities and green advanced extraction technologies of ginger oleoresin extracts: A review. *Food Research International*, 164, 112283.

Kyrana, V.R., Lougovois, V.P., Valsamis, D.S. (1997). Assessment of shelf-life of maricultured gilthead sea bream (Sparus aurata) stored in ice. *International Journal of Food Science & Technology*, 32(4), 339-347.

Laelago Ersedo, T., Teka, T.A., Fikreyesus Forsido, S., Dessalegn, E., Adebo, J.A., Tamiru, M., Astatkie, T. (2023). Food flavor enhancement, preservation, and bio-functionality of ginger (Zingiber officinale): a review. *International Journal of Food Properties*, 26(1), 928-951.

Li, J., Wang, L., Mu, H., Ren, G., Ge, M., Dong, J., Wang, Q., Sun, J. (2024). Effect of 6-gingerol on oxidative stability and quality characteristics of mutton meatballs during refrigerated storage. *Food Chemistry: X*, 24, 101865.

Li, Y., Wu, C., Wu, T., Wang, L., Chen, S., Ding, T., Hu, Y. (2018). Preparation and characterization of citrus essential oils loaded in chitosan microcapsules by using different emulsifiers. *Journal of Food Engineering*, 217, 108-114.

Lian, F., Cheng, J.H., Ma, J., Sun, D.W. (2023). LF-NMR and MRI analyses of water status and distribution in pork patties during combined roasting with steam cooking. *Food Bioscience*, 56, 103325.

Nami, B., Tofighi, M., Molaveisi, M., Mahmoodan, A., Dehnad, D. (2023). Gelatin-maltodextrin microcapsules as carriers of vitamin D3 improve textural properties of synbiotic yogurt and extend its probiotics survival. *Food Bioscience*, 53, 102524.

Nasab, Z.M., Habibi, A. (2024). Microencapsulation of ginger oleoresin through the complex coacervates of gum Arabic and soy protein isolate as the wall materials. *Biocatalysis and Agricultural Biotechnology*, 58, 103179.

Nguyen, C.T., Di, K.N., Phan, H.C., Kha, T.C., Nguyen, H.C. (2024). Microencapsulation of noni fruit extract using gum arabic and maltodextrin - Optimization, stability and efficiency. *International Journal of Biological Macromolecules*, 269, 132217.

Qiu, L., Zhang, M., Adhikari, B., Chang, L. (2022). Microencapsulation of Rose Essential Oil Using Perilla Protein Isolate-Sodium Alginate Complex Coacervates and Application of Microcapsules to Preserve Ground Beef. *Food and Bioprocess Technology*, 16(2), 368-381.

Rahim, M.A., Imran, M., Ambreen, S., Khan, F.A., Regenstein, J.M., Al-Asmari, F., Mohamed Ahmed, I. A. (2023). Stabilization of the Antioxidant Properties in Spray-Dried Microcapsules of Fish and Chia Oil Blends. *ACS Omega*, 8(38), 35183-35192.

Rialita, T., Nurhadi, B., Puteri, R.D. (2018). Characteristics of microcapsule of red ginger (Zingiber officinale var. Rubrum) essential oil produced from different Arabic gum ratios on antimicrobial activity toward Escherichia coli and Staphylococcus aureus. *International Journal of Food Properties*, 21(1), 2500-2508.

San, S.M., Jaturanpinyo, M., Limwikrant, W. (2022). Effects of Wall Material on Medium-Chain Triglyceride (MCT) Oil Microcapsules Prepared by Spray Drying. *Pharmaceutics*, 14(6), 1281.

Sang, S., Snook, H.D., Tareq, F.S., Fasina, Y. (2020). Precision Research on Ginger: The Type of Ginger Matters. *Journal of agricultural and food chemistry*, 68(32), 8517-8523.

Setyaningsih, D., Kurniawan, D., Muna, N. (2020). Encapsulation of ginger oleoresin with a combination of maltodextrin and skim milk powder as wall material. *IOP Conference Series: Earth and Environmental Science*, 472(1), 012016.

Tahir, A., Ahmad, R.S., Khan, M.K., Imran, M., Hailu, G.G. (2024). Optimization of Production Parameters for Fabrication of Gum Arabic/Whey Protein-Based Walnut Oil Loaded Nanoparticles and Their Characterization. *ACS Omega*, 9(21), 22839-22850.

Wang, H.H., Li, M.Y., Dong, Z.Y., Zhang, T.H., Yu, Q.Y. (2021). Preparation and Characterization of Ginger Essential Oil Microcapsule Composite Films. *Foods*, 10(10), 2268.

Wang, J., Li, L., Li, Y., Song, Q., Hu, Y., Wang, Q., Lu, S. (2025). Characterization of thyme essential oil microcapsules and potato starch/pectin composite films and their impact on the quality of chilled mutton. *Food Chemistry*, 464, 141692.

Wang, X., Ding, Z., Zhao, Y., Prakash, S., Liu, W., Han, J., Wang, Z. (2021). Effects of lutein particle size in embedding emulsions on encapsulation efficiency, storage stability, and dissolution rate of microencapsules through spray drying. *Lwt*, 146, 111430.

Wangkulangkool, M., Ketthaisong, D., Tangwongchai, R., Boonmars, T., Lomthaisong, K. (2023). Microencapsulation of Chia Oil Using Whey Protein and Gum Arabic for Oxidation Prevention: A Comparative Study of Spray-Drying and Freeze-Drying Methods. *Processes*, 11(5), 1462.

Xu, T., Gao, C., Feng, X., Yang, Y., Shen, X., Tang, X. (2019). Structure, physical and antioxidant properties of chitosan-gum arabic edible films incorporated with cinnamon essential oil. *International journal of biological macromolecules*, 134, 230-236.

Xu, Y., Feng, H., Zhang, Z., Zhang, Q., Tang, J., Zhou, J., Peng, W. (2023). The Protective Role of Scorias spongiosa Polysaccharide-Based Microcapsules on Intestinal Barrier Integrity in DSS-Induced Colitis in Mice. *Foods*, 12(3), 669.

Yang, X., Shen, J., Liu, J., Yang, Y., Hu, A., Ren, N., Liu, W. (2022). Spray-Drying of Hydroxypropyl β-Cyclodextrin Microcapsules for Co-Encapsulation of Resveratrol and Piperine with Enhanced Solubility. *Crystals*, 12(5), 596.

Yang, X., Zhang, S., Lei, Y., Wei, M., Liu, X., Yu, H., Xie, P., Sun, B. (2023). Preservation of stewed beef chunks by using calcium propionate and tea polyphenols. *Lwt*, 176, 114491.

Zhang, X., Zhang, B., Ge, X., Shen, H., Sun, X., Zhang, Q., Li, W. (2022). Fabrication and Characterization of Whey Protein-Citrate Mung Bean Starch-Capsaicin Microcapsules by Spray Drying with Improved Stability and Solubility. *Foods*, 11(7), 1049.

Zhang, Z.H., Yu, B., Xu, Q., Bai, Z., Ji, K., Gao, X., Xiao, R. (2022). The Physicochemical Properties and Antioxidant Activity of Spirulina (Artrhospira platensis) Chlorophylls Microencapsulated in Different Ratios of Gum Arabic and Whey Protein Isolate. *Foods*, 11(12), 1809.

Acknowledgments

This work was supported by the Science Foundation of Heilongjiang Province, China (grant no. H2018001), the Fundamental Research Funds for the Central Universities (grant no. 2572018BU03) and the Heilongjiang Postdoctoral (grant no. LBH-Z10282).